Rogić and Gagić. Scr Med 2022 Dec;53(4):271-9. DOI:10.5937/scriptamed53-40866
ORIGINAL ARTICLE

3D-QSAR-Based Pharmacophore Determination and Design of Novel DPP-4 Inhibitors

Sanja Rogić,[1] Žarko Gagić[2]

1. Regulatory, Medical and Clinical Affairs, Hemofarm d.o.o. Banja Luka, Banja Luka, the Republic of Srpska, Bosnia and Herzegovina.
2. Department of Pharmaceutical Chemistry, Faculty of Medicine, University of Banja Luka, Banja Luka, the Republic of Srpska, Bosnia and Herzegovina.

Abstract

Background/Aim: Therapy of diabetes mellitus type 2 includes drugs that act as inhibitors of dipeptidyl peptidase 4 (DPP-4) enzyme. Several DPP-4 inhibitors are marketed today and although they have favourable safety profile and tolerability, they show moderate activity in controlling glycaemia. The 3D quantitative structure-activity relationship (3D-QSAR) methodology was employed in order to find pharmacophore responsible for good DPP-4 inhibitory activity and designed new compounds with enhanced activity.
Methods: For 3D-QSAR model development, 48 compounds structurally related to sitagliptin were collected from ChEMBL database. Structures of all compounds were optimised in order to find the best 3D conformations prior to QSAR modelling. To establish correlation between structure and biological activity Partial Least Squares (PLS) regression method integrated in Pentacle software was used.
Results: Parameters of internal and external validation (R^2 = 0.80, Q^2 = 0.64 and R^2_{pred} = 0.610) confirmed reliability of developed QSAR model. Analysis of obtained structural descriptors enabled identification of key structural characteristics that influenced DPP-4 inhibitory activity. Based on that information, new compounds were designed, of which 35 compounds had a better predicted activity, compared to sitagliptin.
Conclusion: This QSAR model can be used for DPP-4 inhibitory activity prediction of structurally related compounds and resulting pharmacophore contains information useful for optimisation and design of new DPP-4 inhibitors. Finally, authors propose designed compounds for further synthesis, *in vitro* and *in vivo* testing, as new potential DPP-4 inhibitors.

Key words: Diabetes; Gliptins; Quantitative structure-activity relationship; Pharmacophore; Molecular design.

Correspondence:
ŽARKO GAGIĆ
E: zarko.gagic@med.unibl.org

ARTICLE INFO

Received: 28 October 2022
Revision received: 15 December 2022
Accepted: 15 December 2022

Introduction

Diabetes mellitus type 2 (DMT2) is a chronic metabolic disorder characterised by hyperglycaemia that is caused mainly by insulin resistance and/or impaired insulin secretion. It is estimated that about 90 % of diabetic patient suffer from type 2 diabetes and its prevalence has been increasing steadily over the years, becoming a global health problem.[1] Prediction of International Diabetes Federation (IDF) is that by the year of 2040, the number of patients with diabetes will rise to around 640 million.[2]

Therapy of DMT2 includes drugs with different mechanisms of action and chemical structures, such as biguanides, sulfonylurea derivatives (first, second and third generation), meglitinides,

This article should be cited as follows: Rogić S, Gagić Ž. 3D-QSAR-based pharmacophore determination and design of novel DPP-4 inhibitors. Scr Med 2022 Dec;53(4):271-9.

α-glucosidase inhibitors, thiazolidinediones, insulin and its analogues, sodium-glucose cotransporter-2 (SGLT2) inhibitors, glucagon-like peptide-1 (GLP-1) receptor agonists, dipeptidyl peptidase 4 (DPP-4) enzyme inhibitors.[3]

DPP-4 inhibitors (also called gliptins) are relatively new class of antidiabetic drugs, which achieve satisfactory therapeutic efficiency. These drugs are generally well tolerated and do not carry a significant risk of hypoglycaemia and weight gain.[4, 5] DPP-4 is a transmembrane glycoprotein that belongs to the group of serine proteases. This exopeptidase catalyses the cleavage of the dipeptide from the N-terminal end of the substrate, leading to its inactivation or generation of new bioactive metabolites. It is a ubiquitous enzyme, found in many cells and tissues and since it shows affinity for different substrates, it can participate in a large number of physiological processes, including inflammation, cardiovascular function and immunity.[6, 7] Increased activity of this enzyme has been found in various diseases such as DMT2, atherosclerosis, diabetic kidney disease etc.[8-10] DPP-4 has been important target for the treatment of DMT2 because of its effect on glucose control via metabolic inactivation of gastrointestinal incretins.[11]

Gastrointestinal incretins, glucagon-like peptide 1 (GLP-1) and glucose-dependent insulinotropic peptide (GIP), play a very important role in the process of establishing blood glucose homeostasis.[12] GLP-1 and GIP are released from L and K intestinal cells, respectively, in response to nutrient ingestion (primarily fat and glucose). They enhance glucose-stimulated insulin secretion from β-cells of the pancreas in an additive manner and inhibit glucagon secretion from α-cells, thereby improving glycaemia. GLP-1 has additional beneficial effects in the gastrointestinal tract such as delayed gastric emptying and reducing appetite, which also contribute to promoting normoglycemia.[13] The DPP-4 enzyme catalyses the cleavage of incretins from the N-terminal end, thus shortening their half-life. Inhibition of DPP-4 is used in therapy of DMT2 to prolong effect of these incretins and lower blood glucose levels.[14] Sitagliptin is first DPP-4 inhibitor introduced in DMT2 therapy in 2006 and since then various DPP-4 inhibitors have been marketed, but research in this area is continuing in an effort to discover more efficient antidiabetic drugs.[15-18]

Computer aided drug design (CADD) comprises various *in silico* techniques that have been used with great success in modern drug discovery process (especially in its early stages) to increase efficiency and save time and money.[19-21] The aim of this study was to employ an *in silico* 3D-quantitative structure-activity relationship study (3D-QSAR) to identify key structural elements that are responsible for DPP-4 inhibitory activity and design new molecules that can lead to discovery of new drugs in therapy of DMT2.

Methods

Data set

The data set comprised 48 compounds that had more than 85 % structural similarity to sitagliptin. The compounds were retrieved from the ChEMBL database, together with their experimentally determined DPP-4 inhibitory activities, expressed as IC_{50} values. For simplicity, those were converted to negative decade logarithm (pIC_{50}), to be further used for QSAR modelling. All activities were determined using the same experimental procedure.

The initial data set was divided into a training set, comprising 35 compounds that were used to build a 3D-QSAR model and a test set, comprising 13 compounds which were used for external validation of the model. Chemical structures of selected compounds from data set that were used for QSAR modelling are depicted in Figure 1.

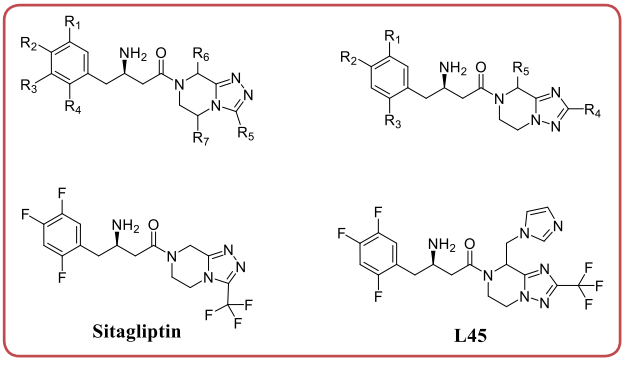

Figure 1: Chemical structures of two class of compounds in data set and their representatives, sitagliptin and compound L45

Before building the QSAR model, the dominant forms at pH 7.4 were determined for all molecules in the MarvinSketch version 6.3.0, ChemAxon (https://www.chemaxon.com). Given that quality of 3D-QSAR model is highly dependent on molecule conformation, the obtained dominant forms were previously subjected to geometrical optimisation in order to achieve the energy minimum. The optimal 3D structures were generated using the PM3 (Parameterised Model Revi-

sion 3) semi-empirical method[22] in the Gaussian 98W program extension[23] incorporated into the Chem3D Ultra 7.0, PerkinElmer (http://www.cambridgesoft.com).

3D-QSAR model development

For 3D-QSAR modelling, the Pentacle version 1.0.6, Molecular Discovery Ltd (https://www.moldiscovery.com/) was used. Unlike other 3D-QSAR methodologies such as CoMFA and CoMSIA, which require prior alignment of molecules to calculate descriptors, Pentacle uses grid-independent descriptors (GRIND).[24] For calculation of these descriptors molecule was placed in 3D-grid and subjected to interactions with different probes that represent most common type of ligand-receptors interactions. These included DRY probe that represent hydrophobic interactions, N1 probe that represents hydrogen bond acceptor (HBA) groups, O probe representing hydrogen bond donors (HBD) and TIP probe describing steric interactions. At each grid point, the steric and electrostatic interactions of attraction and repulsion between the probe and the molecule were calculated, to define molecular interaction fields or MIFs. ALMOND algorithm was then used to extract regions (nodes) that were characterised by most intense favourable interactions for each probe. Number of these extracted nodes was set to 100. Consistently Large Auto and Cross Correlation (CLACC) algorithm was used to transform these nodes into GRIND descriptors that represent distance between same and different nodes. Initial number of calculated descriptors was reduced using fractional factorial design (FFD) method. For correlation between descriptor values and DPP-4 inhibitory activities, Pentacle used Partial Least Squares (PLS) regression. Number of latent variables was set to 5.

Validation of 3D-QSAR model

Validation of the 3D-QSAR model was performed based on internal and external validation parameters. Internal validation was achieved using compounds from training set to obtain following validation parameters: squared correlation coefficient or coefficient of determination (R^2), cross-validated coefficient of determination (Q^2) and Root Mean Square Error of Estimation (RMSEE). The Q^2 parameter was calculated based on the LOO (Leave One Out) method, meaning that one component from the training set was left out each time and a new model was formed from the remaining molecules. This process was repeated until each component from the set was omitted once. Based on the obtained model, the activity of molecules from the training set was predicted and the difference between LOO-predicted and experimental activities $e_{(i)}$ was calculated. The sum of squared $e_{(i)}$ gave PRESS (Predicted Residual Sum of Squares):

$$PRESS = \sum_{i=1}^{n} e_{(i)}^2 \qquad \text{(Eq 1.)}$$

PRESS was used to calculate RMSEE and Q^2:

$$\text{MSEE} = \sqrt{\frac{\text{PRESS}}{n}} \qquad \text{(Eq 2.)}$$

$$Q^2 = 1 - \frac{PRESS}{\sum(Y_{obs\ (training)} - \bar{Y}_{training})^2} \qquad \text{(Eq 3.)}$$

where n represented number of compounds in training set, Y_{obs} was experimentally determined DPP-4 inhibitory activity and $Y_{training}$ was mean value of the experimental activities for the training set.

Model was considered able to reliably predict activity of compounds from training set if: $R^2 > 0.6$, $Q^2 > 0.5$ and RMSEE < 0.5.[25, 26]

Test set was used for external validation of model and calculation of following parameters:

$$R^2_{pred} = 1 - \frac{\sum(Y_{obs\ (test)} - Y_{pred\ (test)})^2}{\sum(Y_{obs\ (test)} - \bar{Y}_{training})^2} \qquad \text{(Eq 4.)}$$

where $Y_{obs\ (test)}$ was experimentally determined DPP-4 inhibitory activity of compounds in test set and $Y_{pred\ (test)}$ predicted inhibitory activity of compounds in test set.

RMSEP value was calculated according to Eq. 2, where n represented number of compounds in test set.

In addition, r_m^2 parameters (r_m^2, $r_m'^2$, $\overline{r_m^2}$ i Δr_m^2) of external validation[27, 28] were calculated. Model was considered able to reliably predict activity of external compounds if: $R^2_{pred} > 0.5$, r_m^2 and $r_m'^2 > 0.5$, difference between them (Δr_m^2) < 0.2 and mean value ($\overline{r_m^2}$) > 0.5.[26, 29]

Results

Using the training set, a 3D-QSAR model was formed, whose predictive power was checked through calculation of internal and external validation parameters. The experimental and predicted activities (pIC_{50}) for the training and test set compounds, together with the calculated validation parameters are presented in Table 1.

Table 1: Experimental and predicted activities of compounds from data set with calculated values of validation parameters

Training set					
Compound	**Experimental pIC_{50}**	**Predicted pIC_{50}**	**Compound**	**Experimental pIC_{50}**	**Predicted pIC_{50}**
L1	7.740	7.648	*L27*	7.520	7.528
L2	7.010	7.102	*L28*	6.720	6.650
L3	7.640	7.521	*L30*	6.290	6.110
L5	6.740	7.141	*L31*	6.090	6.103
L7	7.430	7.438	*L32*	7.090	7.018
L8	7.120	7.114	*L33*	6.570	6.817
L9	7.060	7.182	*L36*	8.300	8.331
L10	7.680	7.403	*L37*	7.040	7.100
L11	5.990	5.935	*L38*	6.680	6.593
L12	6.820	6.763	*L39*	6.110	6.191
L14	7.190	7.270	*L40*	6.940	7.104
L15	7.520	7.278	*L41*	6.880	6.804
L16	6.580	6.582	*L43*	7.150	7.088
L18	7.570	7.696	*L44*	6.760	6.905
L19	7.540	7.476	*L45*	8.700	8.722
L20	6.630	6.563	*L47*	8.400	8.258
L21	6.310	6.389	*L48*	6.480	6.530
L24	6.840	6.964	$R^2 = 0.96$; $Q^2 = 0.71$		
Test set					
Compound	**Experimental pIC_{50}**	**Predicted pIC_{50}**	**Compound**	**Experimental pIC_{50}**	**Predicted pIC_{50}**
L4	8.150	8.633	*L29*	7.220	7.213
L6	5.800	6.651	*L34*	7.060	6.912
L13	6.440	6.769	*L35*	6.910	7.107
L17	6.890	7.000	*L42*	7.040	6.657
L22	6.870	6.994	*L46*	8.400	7.945
L23	7.080	7.131	$RMSEP = 0.396$; $R^2_{pred} = 0.610$		
L25	7.160	7.044	$r^2_m = 0.5525$; $r'^2_m = 0.5023$		
L26	6.660	5.941	$\overline{r^2_m} = 0.5274$; $\Delta r^2_m = 0.0502$		

Table 2: Summary of the most important grid-independent descriptors (GRIND) variables

Variable	Node pair	Distance [Å]	Impact	Description
168	*1N1-N1*	*12.8 - 13.2*	+	*Distance between two HBA.*
210	*TIP-TIP*	*2.4 - 2.8*	+	*Distance between the two steric centres located at the C4 position of the benzene ring.*
281	*DRY-O*	*3.6 - 4*	+	*Distance between the hydrophobic centre such as triazolopyrazine ring and the and the HBD.*
289	*DRY-O*	*6.8 - 7.2*	-	*Distance between the benzene ring and the ammonium ion as HBD.*
347	*DRY-N1*	*2.8 - 3.2*	+	*Distance between the hydrophobic bicycle and the HBA such as triazole nitrogen.*
446	*DRY-TIP*	*15.5 - 15.6*	+	*Distance between the piperazine and the steric centre at the benzene ring.*
457	*DRY-TIP*	*19.6 - 20*	+	*Distance between the triazole and the steric centre at the benzene ring.*
569	*O-TIP*	*10 - 10.4*	-	*Distance between the HBD at the C3 position of butanone and the steric centre at the benzene ring.*
624	*N1-TIP*	*4.8 - 5.2*	-	*Distance between triazole nitrogen and bulky radical, such as trifluoromethyl group, on triazole.*
671	*N1-TIP*	*23.6 - 24*	-	*Distance between HBA and steric centre, not present in all compounds.*

HBA: hydrogen bond acceptor; HBD: hydrogen bond donor;

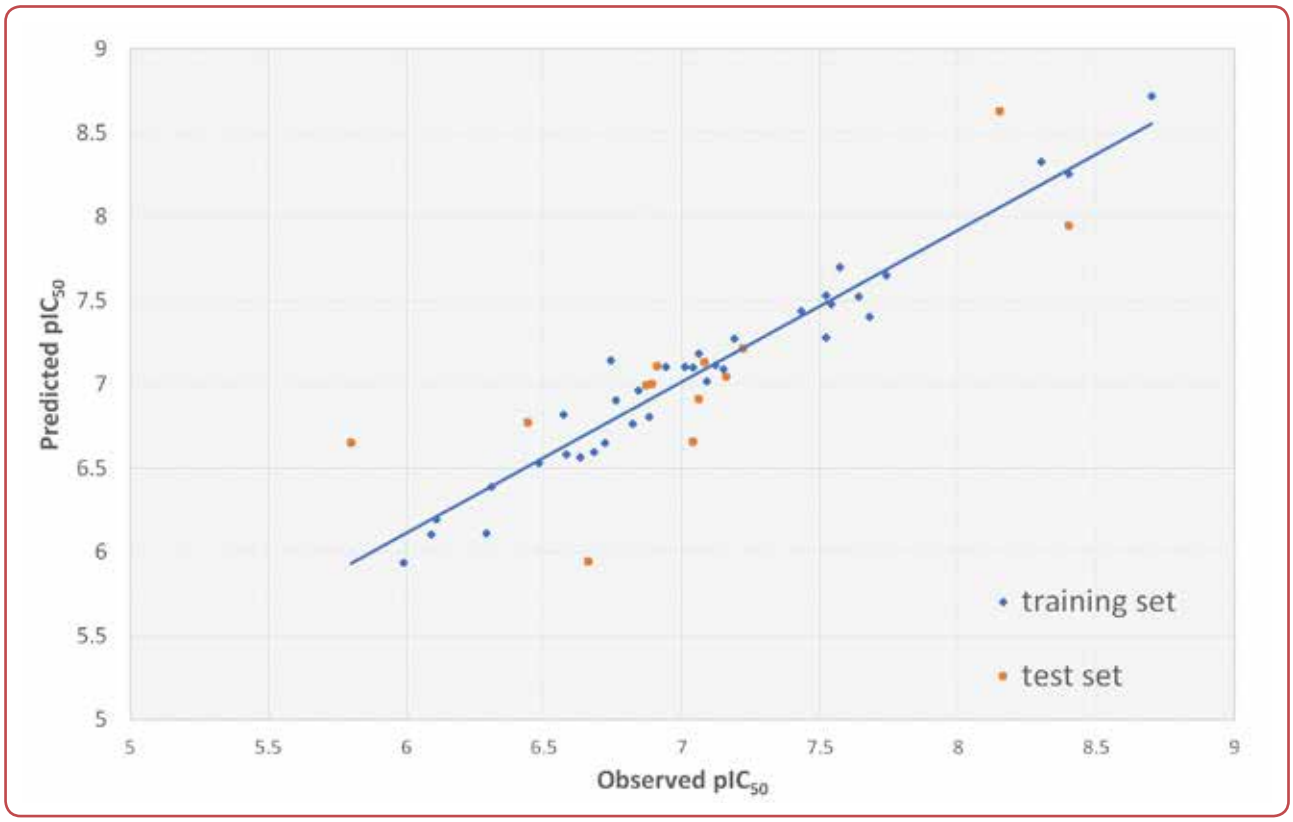

Figure 2: Plot of experimental versus 3D-QSAR predicted DPP-4 inhibitory activities, expressed as pIC_{50} values

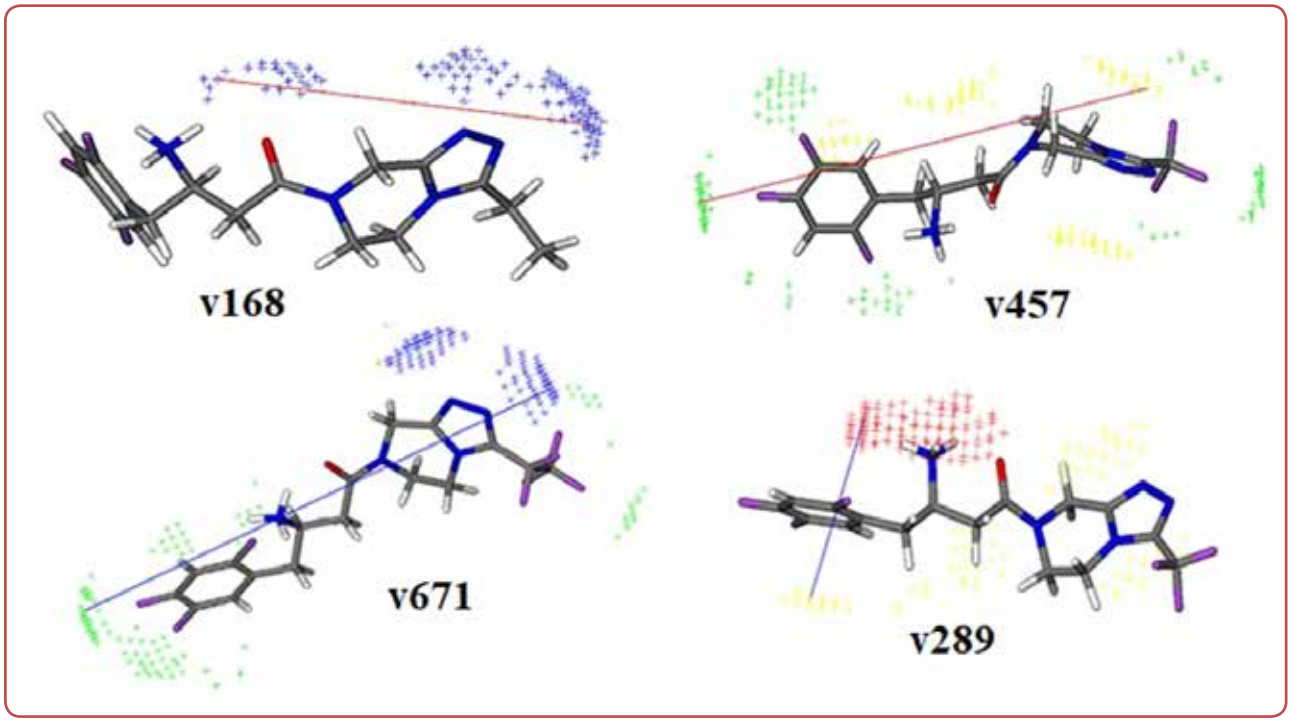

Figure 3: The most important variables that have positive (red) and negative (blue) influence on dipeptidyl peptidase 4 (DPP-4) inhibitory activity. Hydrophobic regions are depicted in yellow, steric hot spots in green, hydrogen bond acceptors (HBA) regions in blue and hydrogen bond donors (HBD) regions in red

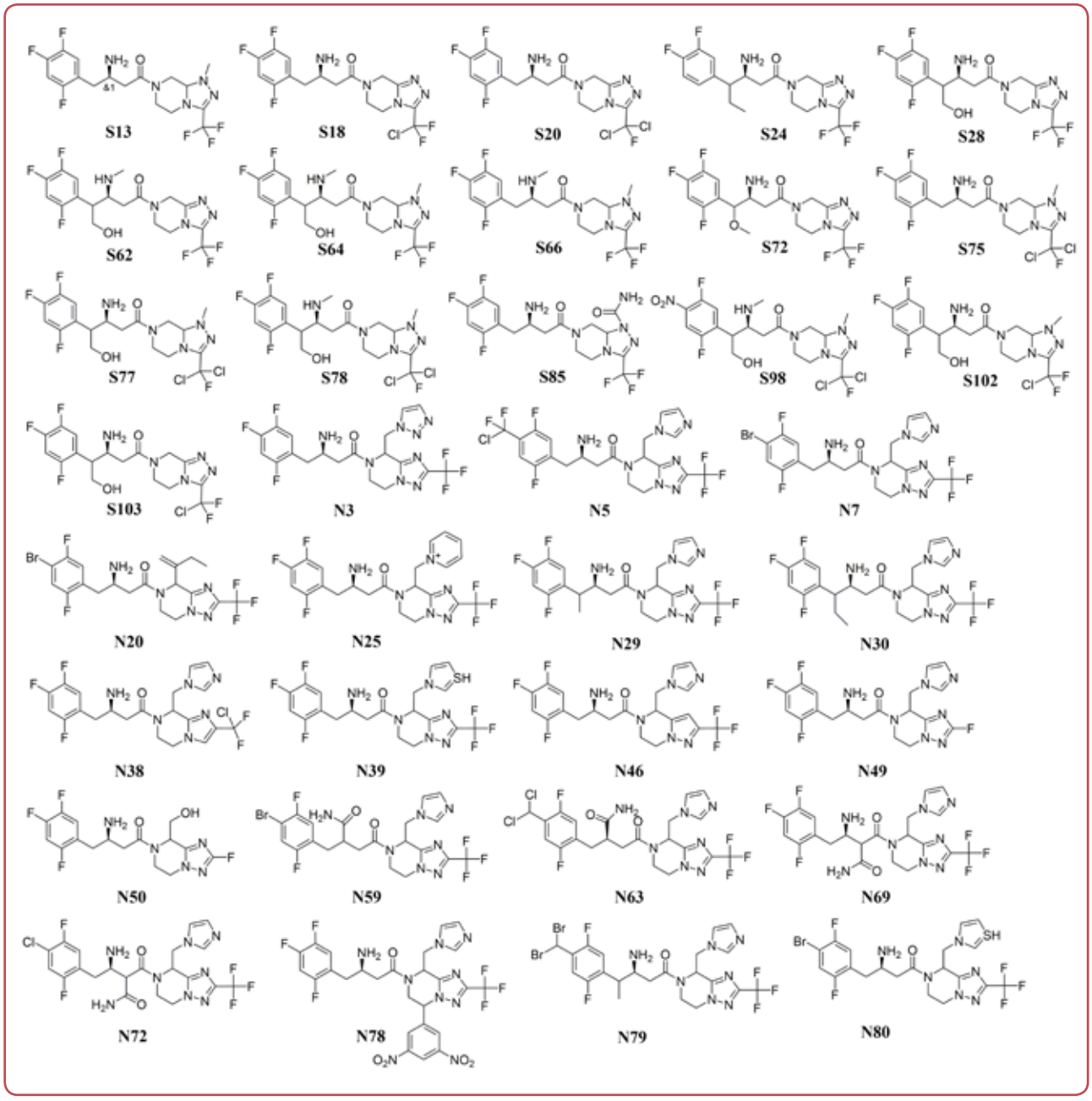

Figure 4: Structures of selected designed compound from S- and N-series with highest predicted dipeptidyl peptidase 4 (DPP-4) inhibitory activity

Table 3: Predicted DPP-4 inhibitory activities of selected designed compounds from S- and N-series

Compound	Experimental pIC_{50}	Compound	Experimental pIC_{50}
S13	*7.762*	*N7*	*8.362*
S18	*7.765*	*N20*	*7.745*
S20	*7.795*	*N25*	*8.201*
S24	*7.818*	*N29*	*8.244*
S28	*7.822*	*N30*	*7.847*
S62	*7.859*	*N38*	*7.805*
S64	*7.895*	*N39*	*8.456*
S66	*8.277*	*N46*	*8.258*
S72	*7.773*	*N49*	*7.764*
S75	*8.230*	*N50*	*7.775*
S77	*7.750*	*N59*	*7.837*
S78	*8.039*	*N63*	*7.806*
S85	*8.178*	*N69*	*7.948*
S98	*7.765*	*N72*	*8.123*
S102	*8.437*	*N78*	*8.174*
S103	*8.354*	*N79*	*7.851*
N3	*7.825*	*N80*	*8.485*
N5	*7.881*		

The good predictive power of the model can be shown in the plot of experimental versus predicted pIC_{50} values (Figure 2) of compounds from training and test set. The even distribution of pIC_{50} values around the regression line indicated a small difference between the experimental and model-predicted values.

The most important variables were selected to explain influence of present structural characteristic on DPP-4 inhibitory activity (Table 2).

Selected variables with positive and negative influence on the activity are presented in Figure 3.

Sitagliptin and compound L45 (Figure 1) were used as lead compounds to design new DPP-4 inhibitors. Two series of compounds were designed, S-series based on sitagliptin structure and N-series based on L45 structure (Figure 4). Activities of designed compounds were predicted using 3D-QSAR model (Table 3).

Discussion

QSAR modelling is one of the most frequently used *in silico* techniques, often applied in the early stages of the discovery of potential drugs, primarily in order to identify, design and optimise lead compounds and to predict toxic properties. Here, 3D-QSAR methodology was used to define key structural determinants that potent DPP-4 inhibitor should possess and that information was used to design new compounds as potential DPP-4 inhibitors. After developing 3D-QSAR model, internal and external validation procedure was performed, in order to demonstrate its reliability. Coefficient of determination parameter (R^2) was calculated which indicates how well the model reproduces the experimental data and Q^2 which is a measure of the model's internal predictive power (Table 1). Values of $R^2 = 0.96$ and $Q^2 = 0.71$ show that model was good at predicting activities of compounds from training set. However, true predictive power of model lies in its ability to predict activities of external compounds that are not used for building the QSAR model. Based on the values of calculated parameters of external validation (Table 1), it can be concluded that this model can be reliably used for that purpose.
In the next step, the interpretation of the obtained GRIND variables was approached (Table 2) in order to define the pharmacophore responsible for the DPP-4 inhibitory activity. That information was used to design new potential DPP-4 inhibitors based on structural modification on sitagliptin (S-series) and compound L45 (N-series), as a compound with the highest activity in data set. Of the 100 designed compounds from S-series, 16 compounds (Figure 4) were predicted to have better activity compared to sitagliptin ($pIC_{50} > 7.740$), while of the 82 designed N-series compounds, 19 compounds (Figure 4) showed better predicted activity compared to sitagliptin (Table 3).

Based on the predicted activities of compounds from S-series it can be concluded that following structural features are essential for good DPP-4 inhibitory activity:

- methyl group at the N1 position of the triazole ring (S-13, S-64, S-66, S-75, S-77, S-78, S-98, S-102);
- methylamino group at the C3 position of the butane chain (S-62, S-64, S-66, S-78, S-98);
- hydroxymethyl group at C4 of the butane chain (S-28, S-62, S-64, S-77, S-78, S-98, S-102, S-103);
- monochloro-/dichloro-fluoromethyl group at the C3 position of the triazole ring, provided that at least two of the aforementioned functional groups are present in the structure (S-75, S-77, S-78, S-98, S-102, S-103). The exception is S-85 with an ureido

group at the N1 position, which significantly increases activity;
- functional groups such as the nitro group at the C4 position of the benzene ring (S-98), ethyl (S-24) and methoxy group (S-72) at the C4 position of the butane chain show moderate increase in activity.

After analysing most active compounds from N-series these structural characteristics were identified as important for high activity:
- bromine at the C4 position of benzene (N-7, N-20, N-59, N-80);
- methylpyridinium ion at position C4 of the condensed cycle (N-25);
- methyl group at the C4 position of the butane chain (N-29, N-79);
- methylthiazole instead of methylimidazole at the C4 position of the condensed cycle (var 624); methylthiazole with bromine at the C4 position of benzene slightly increases activity compared to methylthiazole alone (N-39 and N-80);
- switch of triazolopyrazine bicycle to pyrazolopyrazine (N-46);
- formamide group at the C2 position of the butane chain, provided that the C4 position of benzene is chlorine instead of fluorine; formamide alone does not affect the activity so much (N-69 and N-72);
- 3,5-dinitrophenyl group at the C7 position of the triazolopyrazine (N-78);
- introduction of functional groups such as triazole ring (N-3), difluorochloromethyl (N-5, N-38), dibromomethyl (N-79), dichloromethyl (N-63), hydroxymethyl (N-50), fluorine instead of trifluoromethyl group (N -49, N-50), 2-buten-1-yl (N-20) and ethyl (N-30), leads to a moderate increase in inhibitory activity.

Conclusion

In this study 3D-QSAR methodology was employed in order to define pharmacophore responsible for DPP-4 inhibitory activity and design new compounds with enhanced activity. The reliability of the developed 3D-QSAR model was confirmed by thorough internal and external validation. Guided by the obtained GRIND variables, new compounds were designed by structural modification of the leading molecules sitagliptin and compound L45. Groups that favourably influenced the activity (electronegative sternal group at the C4 position of benzene, donor of hydrogen bonds in the condensed cycle, amino group at the C3 position of the butane chain) were left in the structure. As a result, 35 new compounds with better predicted inhibitory activity compared to sitagliptin, were designed. The modifications that led to an increase in inhibitory activity were the introduction of a methyl group, the substitution of one/two fluorine atoms in the trifluoromethyl group with chlorine, the introduction of hydroxymethyl, ureido groups, changes in the condensed cycle and the introduction of thiazole instead of imidazole in the structure of L45. Results from this study can be used as a basis for further structural modifications and optimisation of designed compounds as new potential DPP-4 inhibitors.

Acknowledgements

This work was a part of the project supported by the Ministry for Scientific-Technological Development, Higher Education and Information Society, the Republic of Srpska, Contract # 19.032/961-149/19.

Conflict of interest

None.

References

1. DeFronzo RA, Ferrannini E, Groop L, Henry RR, Herman WH, Holst JJ, et al. Type 2 diabetes mellitus. Nat Rev Dis Primers 2015;1:15019. doi: 10.1038/nrdp.2015.19.
2. Saeedi P, Petersohn I, Salpea P, Malanda B, Karuranga S, Unwin N, et al. Global and regional diabetes prevalence estimates for 2019 and projections for 2030 and 2045: Results from the International Diabetes Federation Diabetes Atlas, 9(th) edition. Diabetes Res Clin Pract 2019;157:107843. doi: 10.1016/j.diabres.2019.107843.
3. Ko SH, Hur KY, Rhee SY, Kim NH, Moon MK, Park SO, et al. Antihyperglycemic agent therapy for adult patients with type 2 diabetes mellitus 2017: a position statement of the Korean Diabetes Association. Korean J Intern Med 2017;32(6):947-58.

4. Yin R, Xu Y, Wang X, Yang L, Zhao D. Role of dipeptidyl peptidase 4 inhibitors in antidiabetic treatment. Molecules 2022;27(10):3055. doi: 10.3390/molecules27103055.
5. Ahren B. DPP-4 Inhibition and the path to clinical proof. Front Endocrinol 2019;10:376. doi: 10.3389/fendo.2019.00376.
6. Fadini GP, Avogaro A. Cardiovascular effects of DPP-4 inhibition: beyond GLP-1. Vascul Pharmacol 2011;55(1-3):10-6.
7. Tomovic K, Lazarevic J, Kocic G, Deljanin-Ilic M anderluh M, Smelcerovic A. Mechanisms and pathways of anti-inflammatory activity of DPP-4 inhibitors in cardiovascular and renal protection. Med Res Rev 2019;39(1):404-22.
8. Kirino Y, Sato Y, Kamimoto T, Kawazoe K, Minakuchi K. Altered dipeptidyl peptidase-4 activity during the progression of hyperinsulinemic obesity and islet atrophy in spontaneously late-stage type 2 diabetic rats. Am J Physiol Endocrinol Metab 2011;300(2):E372-9.
9. Shibasaki I, Nakajima T, Fukuda T, Hasegawa T, Ogawa H, Tsuchiya G, et al. Serum and adipose dipeptidyl peptidase 4 in cardiovascular surgery patients: influence of dipeptidyl peptidase 4 inhibitors. J Clin Med 2022;11(15):4333. doi: 10.3390/jcm11154333.
10. Daza-Arnedo R, Rico-Fontalvo JE, Pajaro-Galvis N, Leal-Martinez V, Abuabara-Franco E, Raad-Sarabia M, et al. Dipeptidyl peptidase-4 inhibitors and diabetic kidney disease: a narrative review. Kidney Med 2021;3(6):1065-73.
11. Makrilakis K. The role of DPP-4 Inhibitors in the treatment algorithm of type 2 diabetes mellitus: when to select, what to expect. Int J Environ Res Public Health 2019;16(15):2720. doi: 10.3390/ijerph16152720.
12. Nauck MA, Meier JJ. The incretin effect in healthy individuals and those with type 2 diabetes: physiology, pathophysiology and response to therapeutic interventions. Lancet Diabetes Endocrinol 2016;4(6):525-36.
13. Tan Q, Akindehin SE, Orsso CE, Waldner RC, DiMarchi RD, Muller TD, et al. Recent advances in incretin-based pharmacotherapies for the treatment of obesity and diabetes. Front Endocrinol 2022;13:838410. doi: 10.3389/fendo.2022.838410.
14. Drucker DJ, Nauck MA. The incretin system: glucagon-like peptide-1 receptor agonists and dipeptidyl peptidase-4 inhibitors in type 2 diabetes. The Lancet 2006;368(9548):1696-705.
15. Davis JA, Kumar PS, Singh S, Surender A, Roy S, Khanna V, et al. Biological evaluation of RBx-0128, a potent and selective dipeptidyl peptidase-IV inhibitor in type 2 diabetes genetic model. Indian J Pharmacol 2012;44(6):759-64.
16. Kalhotra P, Chittepu V, Osorio-Revilla G, Gallardo-Velazquez T. Structure-activity relationship and molecular docking of natural product library reveal chrysin as a novel dipeptidyl peptidase-4 (DPP-4) inhibitor: an integrated in silico and in vitro study. Molecules 2018;23(6):1368. doi: 10.3390/molecules23061368.
17. Gao Y, Zhang Y, Zhu J, Li B, Li Z, Zhu W, et al. Recent progress in natural products as DPP-4 inhibitors. Future Med Chem 2015;7(8):1079-89.
18. Rogic S, Nukic M, Gagic Z. Quantitative structure-activity relationship study of DPP-4 enzyme inhibitors as drugs in therapy of type 2 diabetes mellitus. In: Badnjevic A, Gurbeta Pokvić L, editors. CMBEBIH 2021: IFMBE Proceedings; 2021 Apr 21-24; Mostar, Bosnia and Herzegovina. Cham: Springer; 2021. p. 481-8.
19. Veselovsky AV, Ivanov AS. Strategy of computer-aided drug design. Curr Drug Targets Infect Disord 2003;3(1):33-40.
20. Javed MR. CADD and molecular dynamic simulations: potential impacts to conventional medicines. Comb Chem High Throughput Screen 2022;25(4):658-9.
21. Sabe VT, Ntombela T, Jhamba LA, Maguire GEM, Govender T, Naicker T, et al. Current trends in computer aided drug design and a highlight of drugs discovered via computational techniques: A review. Eur J Med Chem 2021;224:113705. doi: 10.1016/j.ejmech.2021.113705.
22. Stewart JJP. Optimization of parameters for semiempirical methods I. Method. J Comput Chem 1989;10(2):209-20.
23. Frisch M, Trucks G, Schlegel H, Scuseria G, Robb M, Cheeseman J, et al. Gaussian 98, revision a. 7, Gaussian. Inc, Pittsburgh, PA. 1998;12.
24. Pastor M, Cruciani G, McLay I, Pickett S, Clementi S. GRid-INdependent descriptors (GRIND): a novel class of alignment-independent three-dimensional molecular descriptors. J Med Chem 2000;43(17):3233-43.
25. Gramatica P. On the development and validation of QSAR models. Methods Mol Biol 2013;930:499-526.
26. Tropsha A. Best practices for QSAR model development, validation and exploitation. Mol Inform 2010;29(6-7):476-88.
27. Roy PP, Roy K. On some aspects of variable selection for partial least squares regression models. QSAR Comb Sci 2008;27(3):302-13.
28. Ojha PK, Mitra I, Das RN, Roy K. Further exploring rm2 metrics for validation of QSPR models. Chemometr Intell Lab Syst 2011;107(1):194-205.
29. Pratim Roy P, Paul S, Mitra I, Roy K. On two novel parameters for validation of predictive QSAR models. Molecules 2009;14(5):1660-701.